# Approximations of the generalized Fick-Jacobs equation

Pavol Kalinay[1] and Jerome K. Percus[2,3]
[1]*Institute of Physics, Slovak Academy of Sciences, Dúbravska cesta 9, 84511, Bratislava, Slovakia*
[2]*Courant Institute of Mathematical Sciences, New York University, New York, New York, 10012, USA*
[3]*Department of Physics, New York University, 4 Washington Place, New York, New York 10003, USA*
(Received 22 April 2008; revised manuscript received 23 June 2008; published 5 August 2008)

We analyze the generalized Fick-Jacobs equation, obtained by a rigorous mapping of the diffusion equation in a quasi-one-dimensional (quasi-1D) (narrow 2D or 3D) channel with varying cross section $A(x)$ onto the longitudinal coordinate $x$. We show that for constructing approximations and understanding their applicability in practice, it is crucial to study the 2D (3D) density inside the channel in the regime of stationary flow. We present algorithms enabling us to derive approximate formulas for the effective diffusion coefficient involving derivatives of $A(x)$ higher than $A'(x)$ and give examples for 2D channels. Effects of the boundary conditions at the ends of a finite channel and the case of nonsmooth $A(x)$ are also discussed.

DOI: 10.1103/PhysRevE.78.021103 PACS number(s): 05.40.Jc, 87.10.−e

## I. INTRODUCTION

The study of transport through such complex systems as microporous materials (zeolites, biological membranes) usually requires appropriate simplifications in their description. Many of these can be understood as *dimensional reduction*; a model defined originally on a space of many variables is reformulated as a lower-dimensional or even one-dimensional (1D) problem.

We deal with a simple example of such models: confined diffusion. Consider a narrow 2D or 3D channel with hard reflecting walls, confining noninteracting pointlike particles of density $\rho(x,\mathbf{y},t)$ diffusing inside; $x$ denotes the longitudinal and $\mathbf{y}=(y_1,\ldots)$ the transverse coordinates. In general, one should solve the diffusion equation

$$\partial_t \rho(x,\mathbf{y},t) = D\left(\partial_x^2 + \sum_j \partial_{y_j}^2\right)\rho(x,\mathbf{y},t), \tag{1.1}$$

with some initial condition $\rho(x,\mathbf{y},t)=\rho_0(x,\mathbf{y})$ at time $t=0$, Neumann boundary condition (BC) on the walls, and unspecified BC at the ends of the channel; $D$ denotes the diffusion constant. As usually only movement of the particles along the narrow channel is interesting, we ask whether this task can be formulated as purely one dimensional—i.e., whether there is some partial differential equation (PDE)

$$\partial_t p(x,t) = \hat{Q}(x,\partial_x)p(x,t) \tag{1.2}$$

governing the 1D density $p(x,t)$, defined as $\rho(x,\mathbf{y},t)$ integrated over the local cross section $A(x)$,

$$p(x,t) = \int_{A(x)} \rho(x,\mathbf{y},t)d\mathbf{y}, \tag{1.3}$$

with the spatial operator $\hat{Q}$ acting only upon the longitudinal coordinate $x$. We demand the same result seen in 1D; one should get the same $p(x,t)$ either by solving first Eq. (1.1) starting from some $\rho_0(x,\mathbf{y})$ and then calculating $p(x,t)$ according to (1.3) or calculating first the 1D initial condition $p_0(x)$ for $\rho_0(x,\mathbf{y})$ substituted in (1.3) and then solving Eq. (1.2). The goal is to find such $\hat{Q}$ that this request is met (at least) for some reasonably wide class of initial conditions $\rho_0(x,\mathbf{y})$.

This task becomes nontrivial due to nonhomogeneity of the channel if the cross section $A(x)$ is not constant. The simplest approximation of (1.2) is known for decades as the Fick-Jacobs (FJ) equation [1]

$$\partial_t p(x,t) = D\partial_x A(x)\partial_x(p(x)/A(x)). \tag{1.4}$$

This approximation is not satisfactory in many cases, and so improvements were looked for especially during recent years. We mention the correction derived by Zwanzig [2],

$$\partial_t p(x,t) = D\partial_x A(x)[1 - A'^2(x)/3]\partial_x(p(x)/A(x)),$$

$$\partial_t p(x,t) = D\partial_x A(x)[1 - R'^2(x)/2]\partial_x(p(x)/A(x)), \tag{1.5}$$

for 2D and symmetric 3D channels; $R(x)$ is the radius of the channel and $A(x)=\pi R^2(x)$ in the 3D case. Tests on exactly solvable geometries exhibited improvement only in regions of small $|A'(x)|$, indicating that this correction is only the first term of some series.

Reguera and Rubí [3] presented consistent arguments coming from mesoscopic nonequilibrium thermodynamics to suggest that the corrected FJ equation has the form

$$\partial_t p(x,t) = \partial_x A(x)D(x)\partial_x(p(x,t)/A(x)), \tag{1.6}$$

with an effective diffusion coefficient $D(x)$, a function, whose physical interpretation is well understood, but it cannot be fixed from this phenomenological theory.

A procedure for systematic calculation of the spatial operator $\hat{Q}$ was proposed in [4–6]. By introducing anisotropy in Eq. (1.1) and supposing the transverse diffusion coefficient $D_y \gg D$, we gain a small parameter $\epsilon=D/D_y$, in which we can express iteratively the perturbation expansion of $\hat{Q}(x,\partial_x)$ up to an arbitrary order [4]. The generalized FJ equation then has the form

$$\partial_t p(x,t) = \partial_x A(x)[1 - \epsilon\hat{Z}(x,\partial_x)]\partial_x(p(x,t)/A(x)), \tag{1.7}$$

where

 

$$\hat{Z}(x,\partial_x) = \frac{1}{3}A'^2 + \frac{\epsilon}{45}[A'(A^2A^{(3)} + AA'A'' - 7A'^3) + (A^2A'^2)'\partial_x] + \cdots \quad (1.8)$$

for the 2D case and

$$\hat{Z}(x,\partial_x) = \frac{1}{2}R'^2 + \frac{\epsilon}{48}[R'(R^2R^{(3)} + RR'R'' - 14R'^3) + (R^2R'^2)'\partial_x] + \cdots \quad (1.9)$$

for symmetric 3D channels; we put $D=1$ in our considerations. The parameter $\sqrt{\epsilon}$ has the meaning of a scaling factor of the transverse lengths [$y$ and $A(x)$ in 2D and $R(x)$ in 3D geometry]; small $\epsilon$ corresponds to a channel narrow compared with the scale of variation of the cross section, and this determines the form of the $\hat{Z}$ expansion.

Finally, we can return to the isotropic case and take $\epsilon=1$. Notice that infinitely fast transverse diffusion ($\epsilon=0$) generates the FJ equation and the term $\sim\epsilon^1$ recovers the Zwanzig's correction (1.5). As shown in [5], the first-order correction in (1.7), independently of dimension and cross-sectional shape, involves no further derivatives, but changes the prefactor $A(x)$ in the FJ equation (1.4) to one of the form (1.5). This serves as a strong *a posteriori* justification for (1.6) as a leading approximation.

Equation (1.7) represents an exact dimensional reduction of the original diffusion equation [5]. Nevertheless, it is hard to use it directly in calculations—the higher-order terms are very complicated to be expressed explicitly. In addition, instead of an expected *function* $D(x)$, we have *an operator* $1-\epsilon\hat{Z}(x,\partial_x)$ in Eq. (1.7); the spatial operator $\hat{Q}$ contains derivatives in $x$ of an arbitrary order.

Still, the exact generalized FJ equation (1.7) becomes the phenomenological one (1.6) in the regime of stationary flow and the function $D(x)$ can then be fixed unambiguously using the $\epsilon$ expansion of $\hat{Z}(x,\partial_x)$ [6]:

$$D(x) = 1 - \frac{\epsilon}{3}A'^2 + \frac{\epsilon^2A'}{45}(9A'^3 + AA'A'' - A^2A^{(3)}) - \frac{\epsilon^3A'}{945}(135A'^5 + 45AA'^3A'' - 58A^2A'A''^2 - 41A^2A'^2A^{(3)} - 12A^3A''A^{(3)} + 8A^3A'A^{(4)} + 2A^4A^{(5)}) + \cdots \quad (1.10)$$

for the 2D case and

$$D(x) = 1 - \frac{\epsilon}{2}R'^2 + \frac{\epsilon^2R'}{48}(18R'^3 + 3RR'R'' - R^2R^{(3)}) + \cdots \quad (1.11)$$

for symmetric 3D channels. If $A''$ ($R''$) and all higher derivatives are neglected, the coefficients to any order of $\epsilon$ can be expressed explicitly and the infinite series are summed to

$$D(x) = \frac{\arctan\sqrt{\epsilon}A'}{\sqrt{\epsilon}A'}, \quad D(x) = \frac{1}{\sqrt{1+\epsilon R'^2}} \quad (1.12)$$

for 2D and 3D, respectively.

The first question which we want to answer in this paper is how to obtain better approximations, including more terms of the expansion (1.10). As an example, we derive here the formula

$$D(x) = AA''[\gamma A'(1+\epsilon A'^2 + \epsilon AA'')\arctan(\sqrt{\epsilon}A')/\arctan(\sqrt{\epsilon}\gamma) + AA'' - A'^2(1+\epsilon A'^2)]^{-1}, \quad (1.13)$$

with $\gamma = \sqrt{(1+\epsilon A'^2)^3 - [1+\epsilon(AA')']^2}/\sqrt{\epsilon}[1+\epsilon(AA')']$, which reproduces also the terms proportional to $A''$ in (1.10).

Recently, the approximation (1.12) was tested numerically by calculations of the mean first-passage time; Berezhkovskii *et al.* [7] simulated diffusing particles in a long conical tube. In spite of linear $R(x)$, satisfying the condition of zero $R''$ and the higher derivatives, they achieved a good agreement with the 3D formula (1.12) only for $R'^2<1$.

Actually, the radius of convergence of the series (1.11) in $\epsilon R'^2$ (for zero $R''$ and the higher derivatives) is unity and one can doubt its utility for large $|R'|$. On the other hand, the same formula for the linear cone of any slope can also be derived nonperturbatively [6], within the variational formalism [8].

Thus, our next task is to do a deeper analysis of applicability of our approximations of the generalized FJ equation. We base it mainly on a study of the full-space density $\rho$, connected with the 1D density $p$ of our interest. Let us stress that the procedure of projecting $\rho$ onto $p$ [5] also involves the backward mapping of $p$ onto a specific subset of solutions $\rho$ of Eq. (1.1), containing no transients (modes decaying quickly in the transverse directions). In the regime of stationary flow, there are no such modes, and any stationary 1D density $p(x)$ corresponds unambiguously to some full space $\rho(x,\mathbf{y})$, which also has to be understood if we are to work only in the 1D picture.

In the following section, we study the mapping $\rho\to p$ and backward for the stationary regime. We draw conclusions which enable us to apply nonperturbative methods for calculating $D(x)$ as well as to analyze applicability of the corresponding approximations.

In Sec. III, we present derivation of the approximations of $D(x)$, which include $A''(x)$ for 2D channels. We test them on exactly solvable examples and analyze the range of their validity and possibility of the next improvements.

In Sec. IV, we discuss the mapping in the case of $A(x)$ with cusps and the effects of BCs at the ends of a finite channel on the resulting $D(x)$.

For simplicity, we restrict our detailed analysis to 2D channels. Our conclusions and the proposed techniques can be extended to more complicated (3D) geometries in a straightforward way.

## II. MAPPING OF THE STATIONARY STATE

To explain the mapping for the stationary state, we have to go through the mapping procedure [4,5] in brief. We consider a 2D channel bounded by the $x$ axis and function $A(x)$; $0<y<A(x)$. Neumann BCs are supposed:

$$\partial_y\rho(x,y,t) = 0|_{y=0}, \quad (2.1)$$

$$\partial_y \rho(x,y,t) = \epsilon A'(x) \partial_x \rho(x,y,t)|_{y=A(x)}.$$

The crucial point of the procedure is the search for two operators: Aside from the operator $\hat{Q}$ (or $\hat{Z}$) of our primary interest, it is necessary to look also for an operator $\hat{\omega}$, mapping the space of 1D densities $p(x,t)$ back onto the space of 2D densities $\rho(x,y,t)=\hat{\omega}(x,y,\partial_x)[p(x,t)/A(x)]$. The operator $\hat{\omega}$ has to satisfy the inverse relation

$$p(x,t) = \int_0^{A(x)} dy\ \hat{\omega}(x,y,\partial_x)[p(x,t)/A(x)] \tag{2.2}$$

for any function $p(x,t)$. Both operators are rewritten as series in $\epsilon$,

$$\hat{\omega}(x,y,\partial_x) = \sum_{j=0}^{\infty} \epsilon^j \hat{\omega}_j(x,y,\partial_x),$$

$$\epsilon \hat{Z}(x,\partial_x) = \sum_{j=1}^{\infty} \epsilon^j \hat{Z}_j(x,\partial_x), \tag{2.3}$$

and the diffusion equation (1.1) with imposed anisotropy is expressed using $p(x,t)$ mapped backward onto the space of 2D densities:

$$\sum_{j=0}^{\infty} \epsilon^{j+1} \left( \partial_t - \partial_x^2 - \frac{1}{\epsilon} \partial_y^2 \right) \hat{\omega}_j(x,y,\partial_x) \frac{p(x,t)}{A(x)} = 0. \tag{2.4}$$

The time derivative $\partial_t$ commutes with the spatial operators, and for $\partial_t p(x,t)$, we use Eq. (1.7) with $\hat{Z}$ expanded in $\epsilon$. Comparing the coefficients at $\epsilon^{j+1}$ in Eq. (2.4), we get the recurrence relation

$$\partial_y^2 \hat{\omega}_{j+1}(x,y,\partial_x) = -\partial_x^2 \hat{\omega}_j(x,y,\partial_x) - \sum_{k=0}^{j} \hat{\omega}_{j-k}(x,y,\partial_x) \frac{1}{A(x)} \partial_x A(x) \hat{Z}_k(x,\partial_x) \partial_x \tag{2.5}$$

coupled with

$$\hat{Z}_j(x,\partial_x)\partial_x = \frac{A'(x)}{A(x)} \hat{\omega}_j(x,A(x),\partial_x) \quad \text{for } j>0, \tag{2.6}$$

coming from the diffusion equation integrated over $y$.

These relations enable us to calculate simultaneously $\hat{\omega}_j$ and $\hat{Z}_j$, starting from $\hat{\omega}_0(x,y,\partial_x)=1$ and $\hat{Z}_0(x,\partial_x)=-1$. Double integration of $\partial_y^2 \hat{\omega}_{j+1}$, fixing the BC $\partial_y \hat{\omega}_{j+1}(x,y,\partial_x)|_{y=0}=0$, and the normalization $\int_0^{A(x)} dy\ \hat{\omega}_j(x,y,\partial_x)=\delta_{j,0}$ follow. Finally, $\hat{Z}_{j+1}(x,\partial_x)$ is found from (2.6).

This scheme leads to the expansion of $\hat{Z}$, Eq. (1.8), which is coupled with the expansion of $\hat{\omega}$ in the form

$$\hat{\omega}(x,y,\partial_x) = 1 + \epsilon \hat{\eta}(x,y,\partial_x)\partial_x, \tag{2.7}$$

$$\begin{aligned}\hat{\eta}(x,y,\partial_x) = {} & \frac{A'}{6A}(3y^2 - A^2) + \epsilon \left[ \frac{y^4}{24A^2}(3A'^2 - 2AA'') \right. \\ & + \frac{y^2}{12}(2AA'' - A'^2) - \frac{A^2}{360}(14AA'' - A'^2) \left. \right] \partial_x \\ & + \epsilon \left[ \frac{y^4}{24A^2} \left( -AA^{(3)} + 4A'A'' - 3\frac{A'^3}{A} \right) \right. \\ & + \frac{y^2}{12} \left( AA^{(3)} - 2A'A'' - \frac{A'^3}{A} \right) \\ & \left. - \frac{A^2}{360} \left( 7AA^{(3)} - 8A'A'' - 19\frac{A'^3}{A} \right) \right] + \cdots,\end{aligned} \tag{2.8}$$

generating unambiguously a specific set of solutions $\rho(x,y,t)$ of the original 2D diffusion equation, corresponding to the 1D dynamics (1.7).

The mapping becomes simpler in the stationary state. If $\partial_t \rho(x,y,t)=0$, the stationary longitudinal flux

$$\begin{aligned} J(x,t) &= -\int_0^{A(x)} \partial_x \rho(x,y,t) dy \\ &= -A(x)[1 - \epsilon \hat{Z}(x,\partial_x)] \partial_x \frac{p(x,t)}{A(x)} = J \end{aligned} \tag{2.9}$$

is constant in $x$ and $t$, and then correspondence with the description of Eq. (1.6) can be established [6]. Requirement of getting the same flux, whether expressed from (1.6),

$$J = -A(x)D(x)\partial_x(p(x)/A(x)), \tag{2.10}$$

or by using (2.9) for any $\partial_x(p(x)/A(x))$, results in the relation defining the effective diffusion coefficient $D(x)$,

$$\frac{1}{D(x)} = A(x)[1 - \epsilon \hat{Z}(x,\partial_x)]^{-1} \frac{1}{A(x)}, \tag{2.11}$$

giving the expansion (1.10). Having $D(x)$, we can also calculate the corresponding 2D stationary density $\rho(x,y)$. For any 1D BCs $p(x_L)$, $p(x_R)$ (or $J$) at the ends of the channel, we get

$$\partial_x(p(x)/A(x)) = -J/[A(x)D(x)] \tag{2.12}$$

from Eq. (2.10) and so

$$\frac{p(x)}{A(x)} = \rho_L - J \int_{x_L}^{x} \frac{dx'}{A(x')D(x')}; \tag{2.13}$$

$\rho_L$ denotes $p(x_L)/A(x_L)$. Using the operator $\hat{\omega}$, Eq. (2.7), we obtain finally the stationary 2D density

$$\rho(x,y) = \rho_L - J \left[ \int_{x_L}^{x} \frac{dx'}{A(x')D(x')} + \epsilon \hat{\eta}(x,y,\partial_x) \frac{1}{A(x)D(x)} \right] \tag{2.14}$$

defined unambiguously as a series in $\epsilon$.

The expression in the square brackets in Eq. (2.14) is a quantity independent of the BC $p(x_L)$ and $J$. Curves of constant $z$,

$$z(x,y) = \int \frac{dx}{A(x)D(x)} + \epsilon\hat{\eta}(x,y,\partial_x)\frac{1}{A(x)D(x)}, \quad (2.15)$$

join the points of equal stationary 2D density, so (2.15) represents a transformation to a curvilinear variable $z=z(x,y)$ connected with the stationary flow, depending only on the geometry of the channel. One can also define a variable $\varphi$ orthogonal to $z$, but we omit now this step, as it is not necessary for our next considerations.

If we substitute for $D(x)$ and $\hat{\eta}(x,y,\partial_x)$ in (2.15) from (1.10) and (2.8), we obtain $z(x,y)$ in the form

$$z(x,y) = \sum_{j=0}^{\infty}\sum_{k=0}^{j} \epsilon^j y^{2k} z_{j,k}(x), \quad (2.16)$$

where the first few coefficients $z_{j,k}$ are

$$z_{0,0}(x) = \int \frac{dx}{A(x)},$$

$$z_{1,0}(x) = \frac{1}{3}\int \frac{A'^2}{A}dx - \frac{A'}{6}, \quad z_{1,1}(x) = \frac{A'}{2A^2},$$

$$z_{2,0}(x) = \frac{1}{45}\int (AA'A^{(3)} - A'^2A'' - 4A'^4/A)dx$$

$$- \frac{1}{360}(7A^2A^{(3)} - 22AA'A'' + 2A'^3),$$

$$z_{2,1}(x) = \frac{1}{12A^2}(A^2A^{(3)} - 4AA'A'' + 2A'^3),$$

$$z_{2,2}(x) = -\frac{1}{24A^4}(A^2A^{(3)} - 6AA'A'' + 6A'^3). \quad (2.17)$$

One can check that Eq. (2.16) with the coefficients (2.17) satisfies the stationary mass conservation $[\partial_x^2 + (1/\epsilon)\partial_y^2]z(x,y)=0$ as well as the boundary condition $\partial_y z(x,y) = \epsilon A'(x)\partial_x z(x,y)|_{y=A(x)}$. Going from the opposite side: if the BCs (2.1) are applied to (2.16), understood as an ansatz for $z=z(x,y)$, we get

$$\sum_{k=1}^{j+1} 2kA^{2k-1}(x)z_{j+1,k}(x) = A'(x)\sum_{k=0}^{j} A^{2k}(x)z'_{j,k}(x), \quad (2.18)$$

in the $j$th order of $\epsilon$; the stationary mass conservation gives

$$z_{j+1,k+1}(x) = -\frac{z''_{j,k}(x)}{2(k+1)(2k+1)} \quad (2.19)$$

at $\epsilon^j y^{2k}$. These conditions represent closed systems of differential equations for groups of coefficients $z_{j,k}(x)$ (formed by $z_{j,0}$ and $z_{j+1,k}$; $k>0$). If solved, we recover (2.17) up to two integration constants, corresponding to $\rho_L$ and $J$, which is consistent with the linear relation between the stationary $\rho$ and $z$ in (2.14).

An example of transformation to $z=z(x,y)$ for the exactly solvable linear cone is given in Appendix A.

*Summary and consequences*. We showed in this section, that the effective diffusion coefficient $D(x)$, which was an unfixed function in the original phenomenological theory [3], becomes a well-defined quantity in the stationary regime (for any stationary flux $J$ flowing through the channel) and it can be expressed unambiguously using the operator $\hat{Z}$, Eq. (2.11), coming from the exact mapping [4–6]. Then, within the mapping procedure, also the stationary 1D density $p(x)$, Eq. (2.13), and the corresponding 2D density $\rho(x,y)$, Eq. (2.14), are fixed up to two (irrelevant) integration constants.

On the other hand, the stationary density $\rho(x,y)$ is a solution of the Laplace equation (for $\epsilon=1$) with the BCs (2.1). So we can avoid the perturbation expansion (1.10) and calculate $D(x)$ directly from the Laplace equation for exactly solvable geometries. Taking its solution $\rho(x,y)$ and integrating $p(x)$ according to (1.3), we get $D(x)$ from (2.10). We use this method for deriving higher-order approximations of $D(x)$ in the next section.

Finally, we showed that the stationary flow defines a curvilinear coordinate system in the channel, depending only on its shape [on $A(x)$]. The longitudinal curvilinear coordinate $z=z(x,y)$ is assigned to the curves (surfaces) of the same stationary density (isodensities). In this curvilinear coordinate system, the 2D density $\rho(x,y)$ becomes a function of the only spatial variable $z$; $\rho(x,y)=\rho(z)$. Of course, the relation between $\rho$ and $z$ in our calculations (2.16) and (2.17) is trivial, $\rho(z)=\rho_L - Jz$. Nevertheless, the important finding is the *existence* of such a coordinate system, independent of $J$ and $\rho_L$. In general, we can hardly use directly the transformation (2.16) and (2.17), but now we are justified to suppose a spatial variable $s$ such that $\rho$ is a function only of $s$. If there is a relation $s=s(z)$, introducing $s$ instead of $z$ does not violate the structure of the (stationary) isodensities in the channel and also $\rho(z)=\rho(z(s))=\tilde{\rho}(s)$.

Supposition of such a coordinate is a crucial point of the variational mapping [8]. We reexamine this method and propose it also for the construction of approximations of $D(x)$. Finally, we show that properties of the curvilinear system are important for understanding and applicability of the approximations of the generalized FJ equation.

## III. APPROXIMATIONS OF $D(x)$

Although the mapping procedure presented above allows us to calculate the expansion of the exact stationary density $\rho(x,y)$ and $D(x)$ up to an arbitrary order in $\epsilon$ for any analytic function $A(x)$, it is more convenient in practice to have formulas in a compact form. Tests show [2] that even simple approximate formulas can give more usable results than the truncated series. One way is to sum an infinite subgroup of terms of the exact expansion; e.g., summing the terms depending only on $A'(x)$ gives (1.12). Finding a larger summable subgroup of terms may be difficult.

Another way is to use nonperturbative methods. First, we apply a procedure based on replacing the real boundary $y=A(x)$ by a boundary of some exactly solvable geometry in the vicinity of a chosen $x=\bar{x}$. For the 2D stationary density $\rho(x,y)$ in this geometry, we integrate $p(x)$ and gain $D(x)$ from (2.10).

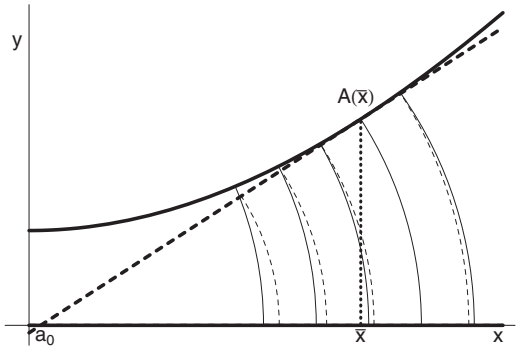


FIG. 1. Linear approximation takes the linearized boundary (thick dashed line) instead of $A(x)$ in the vicinity of a chosen $x=\bar{x}$. So the real isodensities (solid lines) are replaced by the circles (dashed lines), corresponding to the 2D density in the linear cone.

### A. Linear approximation

The simplest approximation of that kind replaces $A(x)$ by its tangent $\bar{A}(x)=\gamma(x-a_0)$ at $x=\bar{x}$ (Fig. 1), where

$$\gamma = A'(\bar{x}), \quad a_0 = \bar{x} - A(\bar{x})/A'(\bar{x}). \tag{3.1}$$

True isodensities (solid lines) are approximated by a system of concentric circles (dashed lines), which depict the 2D density $\rho(x,y)=\rho_L - C\ln[(x-a_0)^2+y^2]$ in a linear cone (bounded by the thick dashed line and $x$ axis) with particles imposed steadily at the point $(a_0,0)$ and diffusing inside the cone to infinity. If we fix the constant $C$ to fit the flux $J=-\int_0^{\bar{A}(x)} dy\, \partial_x \rho(x,y)$, we arrive at the stationary density (A2) for $\epsilon=1$:

$$\rho(x,y) = \rho_L - \frac{J}{2\arctan\gamma}\ln[(x-a_0)^2+y^2]. \tag{3.2}$$

Now, integrating (3.2) over the approximated cross section, we get the stationary 1D density

$$p(x) = \int_0^{\bar{A}(x)} \rho(x,y)dy = \gamma(x-a_0)\left[\rho_L - \frac{J}{\arctan\gamma} \times \left(\frac{\arctan\gamma}{\gamma} - 1 + \ln[\sqrt{1+\gamma^2}(x-a_0)]\right)\right] \tag{3.3}$$

entering the formula (2.10). If the linearized boundary $\bar{A}(x)$ instead of $A(x)$ is used there, too, the relation

$$\bar{A}(x)\partial_x \frac{p(x)}{\bar{A}(x)} = -\frac{J\gamma}{\arctan\gamma} = -\frac{J}{D(x)} \tag{3.4}$$

immediately gives $D(x)=(\arctan\gamma)/\gamma=(\arctan A')/A'$. We obtained the relation (1.12) for $\epsilon=1$ as $A''$ and the higher derivatives were neglected by linearizing $A(x)$ in this construction. Notice also that the integration constants $\rho_L$ and $J$ are irrelevant in the calculation of $D(x)$.

### B. Circular approximation

Replacing the boundary $y=A(x)$ at $x=\bar{x}$ by a circle $\bar{A}(x)$ (Fig. 2) enables us to gain an approximation involving also

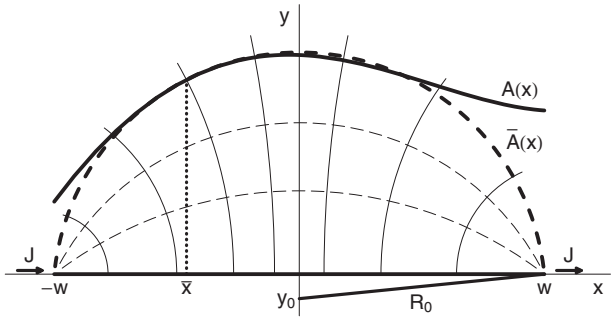


FIG. 2. Approximation of the boundary $y=A(x)$ (thick solid line) at $x=\bar{x}$ by a circle (thick dashed line) of radius $R_0$ and centered at $(0,y_0)$. The thin solid circles represent the isodensities in the circular cavity; the thin dashed lines are circles orthogonal to them.

$A''$ in the final formula for $D(x)$. We utilize here an exactly solvable model supposing that particles are steadily imposed at the point $(-w,0)$ and drained away at $(w,0)$. [The equivalent model in electrostatics supposes a couple of opposite charges placed at $(\pm w,0)$ in the plane; we consider the 2D logarithmic Coulomb potential.] The isodensities are circles (thin solid lines) centered at the $x$ axis; the current flows in the perpendicular direction to them along the thin dashed circles, centered on the $y$ axis at $(0,y_0)$ (for details see Appendix B). So any of the dashed circles can serve as a boundary of a channel and the BCs (2.1) for the corresponding $\rho$ in this model are satisfied. Of course, the origin of the coordinate system can be shifted in the $x$ direction by any $x_0$, so finally, we have three parameters $x_0$, $y_0$, and $w$ (or the radius $R_0=\sqrt{w^2+y_0^2}$) of the circular boundary to be set (keeping the model solvable) to fit $A$, $A'$, and also $A''$ of the true boundary at $x=\bar{x}$. Taking the equation of the approximating circle,

$$[\bar{A}(x)-y_0]^2 + (x-x_0)^2 = R_0^2, \tag{3.5}$$

and the first two derivatives

$$\bar{A}'(x) = \frac{-(x-x_0)}{\bar{A}(x)-y_0}, \quad \bar{A}''(x) = \frac{-R_0^2}{[\bar{A}(x)-y_0]^3}, \tag{3.6}$$

we get three equations for $x_0$, $y_0$, and $R_0$, to be expressed using $\bar{A}(x)=A(x)$, $\bar{A}'(x)=A'(x)$, and $\bar{A}''(x)=A''(x)$ taken at $x=\bar{x}$. The solution reads

$$\bar{x} - x_0 = \frac{A'(\bar{x})}{A''(\bar{x})}[1+A'^2(\bar{x})], \quad R_0^2 = \frac{[1+A'^2(\bar{x})]^3}{A''^2(\bar{x})},$$

$$y_0 = \frac{1}{A''(\bar{x})}[1+A'^2(\bar{x})+A(\bar{x})A''(\bar{x})] \tag{3.7}$$

and

$$w = -\frac{1}{A''}\sqrt{(1+A'^2)^3 - (1+A'^2+AA'')^2}. \tag{3.8}$$

The 2D density in the channel defined by $y=\bar{A}(x)$ and $x$ axis is known,

$$\rho(x,y) = \rho_L - \frac{J}{2 \arctan \gamma} \ln \frac{(w+x-x_0)^2+y^2}{(w-x+x_0)^2+y^2}, \quad (3.9)$$

the prefactor of the logarithm is fixed again from the condition $J=-\int_0^{\bar{A}(x)} dy \partial_x \rho(x,y)$, and $\gamma=-\sqrt{R_0^2-y_0^2}/y_0$. If $\rho$, Eq. (3.9), is integrated over the approximated cross section, we get

$$\frac{p(x)}{\bar{A}(x)} = \rho_L - \frac{J}{\arctan \gamma}\left[\frac{1}{2}\ln\frac{w_+^2+1}{w_-^2+1} + w_+ \arctan(1/w_+) - w_- \arctan(1/w_-)\right], \quad (3.10)$$

$w_\pm=[\sqrt{R_0^2-y_0^2} \pm (x-x_0)]/\bar{A}(x)$. After completing the derivative $[p(x)/\bar{A}(x)]'$, we express the parameters $x_0$, $y_0$, and $R_0$ using $A$, $A'$, and $A''$ at $x=\bar{x}$ according to (3.7), which converts the final formula for $D(x)$ to the form

$$D(x) = -J\{A(x)[p(x)/A(x)]'\}^{-1} = AA''[\gamma A'(1+A'^2+AA'') \times (\arctan A')/(\arctan \gamma) + AA'' - A'^2(1+A'^2)]^{-1}, \quad (3.11)$$

$$\gamma = \frac{\sqrt{(1+A'^2)^3-(1+A'^2+AA'')^2}}{1+A'^2+AA''} \quad (3.12)$$

(at $x=\bar{x}$). Keeping $J=-\int_0^{A(x)} \partial_x \rho(x,y) dy$ requires us to take arctan $\gamma$ from the interval $(\pi/2,\pi)$ for negative $\gamma$. $\gamma$ can be also a pure imaginary number, $\gamma=iu$, $0 \leqslant u < 1$. Then arctan $\gamma = i \ln[\sqrt{(1+u)/(1-u)}]$. The last case corresponds to the approximating circle lying thoroughly above the $x$ axis.

For small $A''$, $\gamma=|A'|-AA''/|A'|+\cdots$, and the leading term of (3.11) expanded in $A''$ recovers the formula (1.12).

If the transverse length $A$ and its derivatives $A'$ and $A''$ are scaled by $\sqrt{\epsilon}$, we arrive at the formula (1.13). In the limit $\epsilon \to 0$, $\gamma \to \sqrt{A'^2-2AA''}$ is finite and arctan$\sqrt{\epsilon}\gamma$ can be replaced by $\sqrt{\epsilon}\gamma$. The leading term of $D(x)$ is unity, as required by the FJ approximation, valid in this limit. The next terms of the Taylor expansion in $\epsilon$ are

$$D(x) = 1 - \frac{\epsilon}{3}A'^2 + \frac{\epsilon^2}{45}A'^2(9A'^2+AA'') - \frac{\epsilon^3}{945}A'^2 \times (135A'^4+45AA'^2A''+5A^2A''^2) + \cdots. \quad (3.13)$$

If compared with (1.10), this approximation sums correctly also the terms proportional to $A''$.

### C. Other approximation

Any exactly solvable geometry with $n$ free parameters $a_1,\ldots,a_n$ can be used for deriving an approximate formula for $D(x)$ by this algorithm; then, the derivatives of $A(x)$ up to $A^{(n-1)}(x)$ will be involved. For 2D channels, formulation in the complex plane offers various possibilities; we present this theory in Appendix B. Here, we pick out only several results for comparison with the linear approximation (LA) and the circular approximation (CA).

The following formulas correspond to approximations of the boundary by solutions $\bar{A}(x)$ of specific polynomial equations, for which the stationary density $\rho(x,y)$ is solvable. In the lowest-order case $n=2$, the approximating boundary is the hyperbola

$$\bar{A}(x) = 1/(a_1+2a_2x). \quad (3.14)$$

Two parameters $a_1$ and $a_2$ allow us to involve only $A$ and $A'$ in the formula (derived by the same algorithm as the CA)

$$\frac{1}{D(x)} = 1 + \frac{1}{3}A'^2(x); \quad (3.15)$$

we get the extrapolation Mod2 in [2]. Although it depend explicitly only on $A'$, it differs from (1.12), because, here, the higher derivatives are not neglected. For the hyperbola (3.14), $\bar{A}''(x)=2\bar{A}'^2(x)/\bar{A}(x)$, and also the higher derivatives can be expressed using $\bar{A}$ and $\bar{A}'$. If these relations are substituted into (1.10), we get an expansion, which is identical (for $\epsilon=1$) with the expansion of $D(x)$ from (3.15) in $A'^2$. It means that Mod2 (in 2D) has a good physical interpretation; it corresponds to approximation of the boundary by hyperbola (3.14).

The approximations for $n=3$,

$$D(x) = \frac{3-A(x)A''(x)-A'^2(x)}{3-A(x)A''(x)-A'^4(x)}, \quad (3.16)$$

and $n=4$,

$$D(x) = 5(9-12A'^2-12AA''+3A'^4+3A^2A''^2-2A^2A'A^{(3)}) \times (45-45A'^2-60AA''-9A'^4+15A^2A''^2 - 21AA'^2A''-9A^2A'A^{(3)}+33A'^6-17AA'^4A'' + 3A^2A'^2A''^2-A^2A'^3A^{(3)})^{-1}, \quad (3.17)$$

involve explicitly also $A''$ and $A^{(3)}$ in the formulas. If we rescale $A$ and its derivatives by $\sqrt{\epsilon}$, the expansion of (3.17) reproduces also the complete term $\sim\epsilon^2$ in (1.10).

Finally, we test the presented results on two exactly solvable geometries. The first one is a 2D hyperbolic cone (Fig. 3)

$$A(x) = \gamma\sqrt{x^2+a^2/(1+\gamma^2)}, \quad (3.18)$$

for which we can find the exact $D(x)$ (Appendix B):

$$\frac{1}{D(x)} = 1 + \frac{\gamma^2x^2}{A^2(x)}\left(\frac{\gamma}{\arctan\gamma}-1\right); \quad (3.19)$$

$\gamma \in (0,\infty)$ characterizes the opening of the cone and $a$ is the transverse length unit. A comparison of our approximations is given in Fig. 4. The CA (thick dotted line) slightly improves the LA (thick dashed line); the thick solid line represents the exact result. The approximation Mod2 by hyperbola (3.15) (thin dashed line) exhibits wrong asymptotics for large $x$. The formula (3.16) gives even worse results and (3.17) has singularities, so they are not plotted in the figure.

The second test is done on a channel shaped by

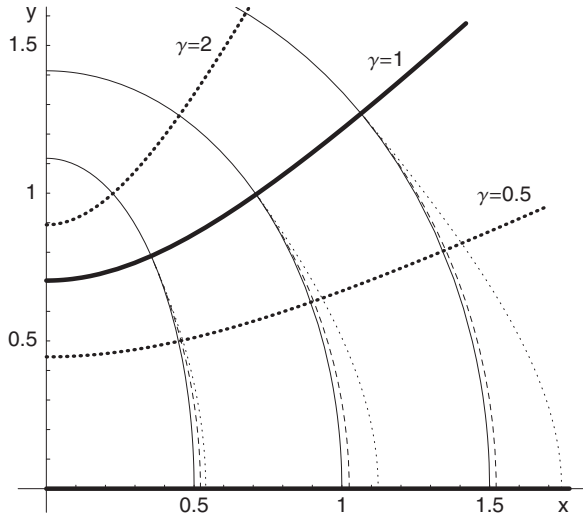


FIG. 3. Hyperbolic cones (3.18) for $a=1$ and various $\gamma$ (the dotted and solid thick lines). The thin solid lines are the exact isodensities for any $\gamma$ (ellipses); the thin dashed lines are circles, replacing the ellipses in the LA and CA; small dots depict hyperbolic isodensities corresponding to the Mod2 approximation (3.15) (drawn for $\gamma=1$).

$$A(x) = \arcsin\left(\frac{g}{\cosh x}\right); \tag{3.20}$$

$0<g\leqslant 1$ (Fig. 5). For $g\to 1$, the bulge at $x=0$ turns to a cusp. Using the algorithm described in Appendix B, we derive

$$\frac{1}{D(x)} = \frac{1}{\cosh^2 x} + \frac{g\tanh^2 x}{\arcsin[g/\cosh(x)]\sqrt{\cosh^2 x - g^2}}. \tag{3.21}$$

The results for $g=0.87$ and 1 obtained by applying all derived formulas for $D(x)$ are depicted in Fig. 6. Also, for this geometry, the numerical results for the CA formula (3.11) (large dotted lines) exhibit almost no change with respect to the much simpler LA formula (1.12) (thick dashed lines). On the other hand, the approximations (3.16) and (3.17) (small dotted and thin solid lines), which were unsuitable for the cone, are much closer to the exact $D(x)$ (thick solid line) in the troubling region $x\sim 0$ for $g=0.87$. The case $g=1$ corresponds to the boundary with a cusp, which makes problems for any formula based on the first few derivatives of $A(x)$. The formula (3.17) becomes unstable, and its data are not plotted.

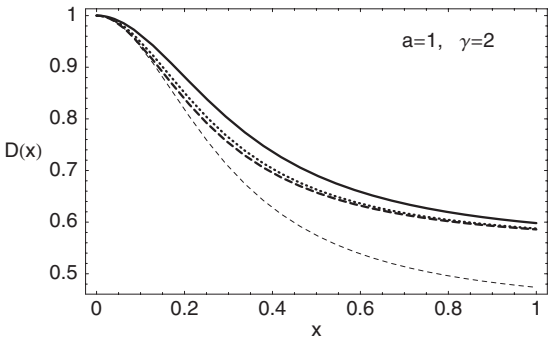


FIG. 4. $D(x)$ for the hyperbolic cone (3.18) for $a=1$ and $\gamma=2$. The solid line represents the exact solution , the thick dashed line is the LA (1.12), and the thick dotted line is the CA (3.11). The thin dashed line depicts Mod 2, Eq. (3.15).

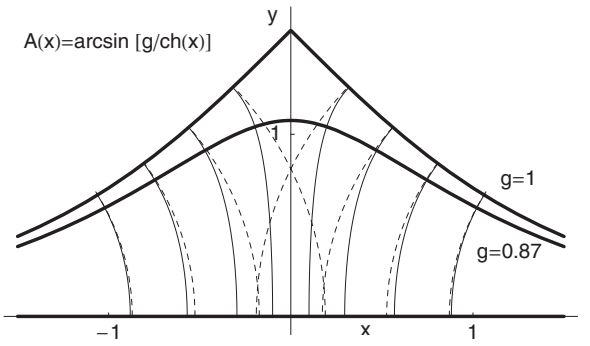


FIG. 5. Testing channels defined by (3.20) (thick lines). The solid thin lines describe the exact isodensities; the dashed lines are the isodensities approximated by circles for $g\to 1$.

Our algorithm of calculating $D(x)$, based on replacing the true boundary by an exactly solvable geometry in the vicinity of a chosen $x$, has a transparent physical interpretation and enables us to obtain higher-order formulas for $D(x)$ with

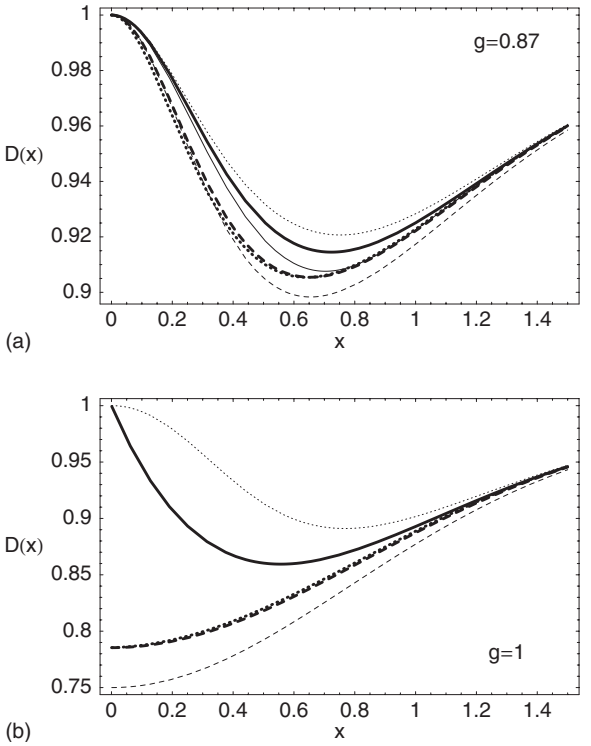


FIG. 6. The effective diffusion coefficient $D(x)$ for the channel bounded by the function (3.20) for $g=0.87$ and 1, calculated by using all derived formulas. The thick solid line is the exact solution (3.21). The thick dashed line is the LA (1.12); the thick dotted line is the CA (3.11). The thin lines depict the approximations (3.15)–(3.17). The approximation by hyperbola (Mod 2 or $n=2$) corresponds to the dashed line; the dotted line plots $n=3$ and the solid line $n=4$.

relative ease. The first problem indicated by solving our examples is that these formulas might not be universal. In contrast to the LA (1.12), certain higher-order approximations are usable only for the channels of specific types (cones, bulges, etc.). Nevertheless, one should have other controls to check how reliable some approximation is.

The basic test is to rescale the transverse lengths [$A(x)$ and its derivatives] by $\sqrt{\epsilon}$ and expand the approximated $D(x)$ in $\epsilon$. After comparison with the exact expansion (1.10), one can see which groups of terms were summed in the formula. Still, the higher derivatives of $A(x)$ are often not neglected, but included implicitly via existing relations between them and the lower-order derivatives, valid on the approximating boundary $y=\bar{A}(x)$, and so this analysis can be biased.

Understanding the applicability of any formula for $D(x)$ requires mainly a study of the 2D stationary density $\rho(x,y)$, corresponding to the approximating exactly solvable geometry, or a study of the corresponding curvilinear coordinate system. From this viewpoint, we can easily explain our test results: in both examples, the CA does not improve markedly $D(x)$ in comparison with the LA (1.12), although it involves correctly $A''$ terms in its expansion. It may be caused by using the same (circular) shape of isodensities. For large $x$ in the hyperbolic cone, the exact (elliptical) isodensities are close to circles (Fig. 3), used by the LA and CA. So both approximations exhibit correct asymptotics, in contrast to Mod 2, Eq. (3.15), which supposes hyperbolic isodensities. On the other hand, the circular isodensities are not capable of fitting the true isodensities in the bulge of the second example (thin solid lines in Fig. 5). In the limit $g\to 1$, the circles (dashed lines) cross one another; the approximated curvilinear coordinate system based on them crashes and so the LA as well as the CA fails.

If the shape of isodensities is so important, one should start by looking for approximations for them instead of first approximating the boundary. In other words, we should find an ansatz for the relation $s=s(x,y)$ such that the 2D density $\rho$ becomes a function of the only spatial variable $s$; $\rho(x,y,t)=\rho(s,t)$ in general. This task is solvable within variational mapping [8], so we reexamine this method in the rest of this section and in Appendix C.

### D. Variational mapping

We start from the functional $F[\rho(x,y,t),\bar{\rho}(x,y,t)]$,

$$F[\rho,\bar{\rho}]=\int_{t_0}^{t_1}dt\int_{x_L}^{x_R}dx\int_0^{A(x)}dy\left(\frac{1}{2}(\bar{\rho}\dot{\rho}-\dot{\bar{\rho}}\rho)+\partial_x\bar{\rho}\partial_x\rho+\frac{1}{\epsilon}\partial_y\bar{\rho}\partial_y\rho\right) \tag{3.22}$$

(keeping the parameter of anisotropy $\epsilon$), whose stationary condition $\delta F[\rho,\bar{\rho}]=0$ generates a pair of diffusion and "antidiffusion" equations

$$\dot{\rho}=\left(\partial_x^2+\frac{1}{\epsilon}\partial_y^2\right)\rho,\qquad -\dot{\bar{\rho}}=\left(\partial_x^2+\frac{1}{\epsilon}\partial_y^2\right)\bar{\rho}, \tag{3.23}$$

governing the evolution of the density $\rho(x,y,t)$, defined in the domain $x_L<x<x_R$, $0<y<A(x)$ in the time $t$ running from $t_0$ to $t_1$, and the complementary function $\bar{\rho}(x,y,t)$, defined in the same domain, but evolving in the time $t$ running backward. In the functional $F$, Eq. (3.22), we complete the integral over the transverse variable *along* the supposed isodensity $s$, obtaining a new functional $F_{1D}[\rho(s,t),\bar{\rho}(s,t)]$. Then, from the stationary condition $\delta F_{1D}=0$, we arrive at the mapped 1D equation for the 2D density $\rho(s(x,y),t)$ in the curvilinear coordinate $s$,

$$\partial_t\rho(s,t)=\frac{1}{\alpha(s)}\partial_s\kappa(s)\partial_s\rho(s,t), \tag{3.24}$$

and its complementary 1D equation for $\bar{\rho}(s,t)$ (unimportant for our next considerations) in a simple FJ form. In the 2D case [8], the functions $\alpha(s)$ and $\kappa(s)$ are given by the relations

$$\alpha(s)=\int_0^{A(x_s)}\frac{\partial x}{\partial s}dy,$$

$$\kappa(s)=\int_0^{A(x_s)}\left(\frac{\partial x}{\partial s}\right)^{-1}\left[1+\frac{1}{\epsilon}\left(\frac{\partial x}{\partial y}\right)^2\right]dy; \tag{3.25}$$

$x=x(s,y)$ is the function inverse to $s=s(x,y)$ and $x_s$ is the $x$ coordinate of intersection of the curve $s=s(x,y)$ with the boundary; $s=s(x_s,A(x_s))$.

The transformation relation $s=s(x,y)$ is understood here as a variational ansatz, unfixed by the method itself. For any choice of $s(x,y)$, this variational technique finds some $\alpha(s)$ and $\kappa(s)$, Eqs. (3.25), optimizing the functional generating the diffusion equation.

Our analysis in Sec. II shows that we are justified to suppose the existence of such a curvilinear coordinate. If $s=z$ of the form (2.16) and the coefficients $z_{j,k}(x)$ are fixed according to (2.17), Eq. (3.24) describes the limit of the stationary flow (slowly changing, but finite fluxes) exactly. The full dynamics is then understood in the background of the curvilinear coordinate system $(z,\varphi)$, generated by the stationary state, and the variational mapping represents an approximation allowing evolution of the density only in the corresponding longitudinal curvilinear coordinate $z$.

For calculations of $D(x)$, we deal only with the stationary regime and our task is to find an ansatz $s=s(x,y)$, approximating properly the isodensities defined by $z=z(x,y)$, Eqs. (2.16) and (2.17). Our goal is to make it flexible enough to fit the true isodensities in various types of channels, but still allowing us to calculate the corresponding $D(x)$ analytically. We present this theory in Appendix C; we demonstrate that the basic approximations, using circles, are the LA and CA, and then we formulate general rules for their next improvements.

## IV. NONSMOOTH BOUNDARIES

The problem of crossing approximate isodensities, visible in Fig. 5 (the dashed lines), when the curves of a chosen approximate form are not able to describe consistently the stationary 2D density inside the channel, appears naturally in the channels of nonsmooth boundaries. The mapping method

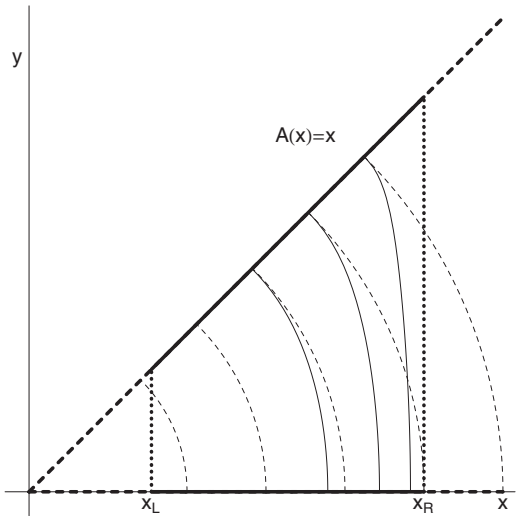


FIG. 7. Finite 2D linear cone bounded by the thick solid lines; $x_L<x<x_R$. The mapping procedure finds the circular (thin dashed lines) isodensities, corresponding to the uncut cone (bounded by the thick dashed lines). The true isodensities (thin solid lines) in the finite cone have to respect the BC at its ends (dotted lines) $\rho(x_{L,R},y)=\rho_{L,R}$, not depending on $y$.

using the operator $\hat{Z}(x,\partial_x)$, Eq. (1.7), supposes that the function $A(x)$ defining the boundary is analytic. Then the isodensities, generated by the mapping in the vicinity of some $x=\bar{x}$, correspond to a channel shaped by the Taylor series of the function $A(x)$ in the neighborhood of $\bar{x}$. Of course, this continuation differs from the real boundary behind a cusp and so the structure of the stationary density obtained by the mapping and finally $D(x)$, too, becomes wrong.

In many cases, the ends of the channel also behave like nonanalytic points. The stationary density calculated by the mapping procedure corresponds to an infinite channel continuing behind its ends $x_L$ and $x_R$ according to the Taylor series of the function shaping its boundary. If the imposed boundary conditions at the ends $\rho(x_L,y)$ and $\rho(x_R,y)$ do not fit the stationary density at $x=x_{L,R}$ in the uncut channel, then the true $D(x)$ differs from that one obtained by the mapping procedure.

*An example: finite linear cone*. Consider a 2D linear cone with $A(x)=\gamma x$, where $x$ is restricted by $0<x_L<x<x_R$ (Fig. 7). In the uncut cone (beginning at $x=0$), the mapping generates the stationary density $\rho(x,y)=\rho_L-(J/2\arctan\gamma)\ln(x^2+y^2)$ according to (A2), giving $D(x)=(\arctan\gamma)/\gamma$, which is the exact result for this geometry for any $\gamma$. The usual BCs for the finite cone, imposing constant densities at the ends $\rho(x_{L,R},y)=\rho_{L,R}$ (along the dotted lines in Fig. 7), do not fit the circular isodensities, appearing in the uncut cone, and so the corresponding $D(x)$ differs from (1.12).

The case of $x_L=0$ and $\gamma=1$ can be easily calculated by the method of images. An infinite lattice of sources and sinks at the points $(2nx_R,2mx_R)$ with integer $n$ and $m$ (the sources placed at even $n+m$ and the sinks at odd $n+m$) generates the correct BC at the boundary $x=x_R$; $\rho(x_R,y)=\text{const}$. The 2D density is then

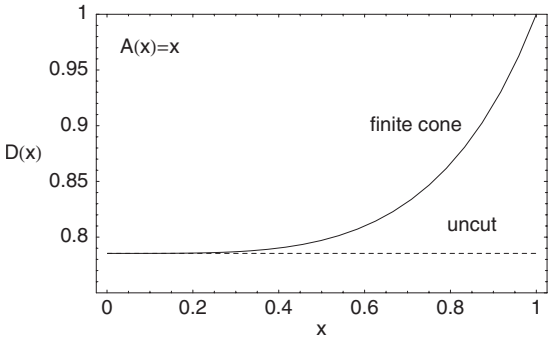


FIG. 8. Effective diffusion coefficient $D(x)$ for the finite linear cone $A(x)=x$; $0<x<1$ (solid line) compared with the exact result for the uncut cone (dashed line), the constant $D(x)=\pi/4$.

$$\rho(x,y)=-\frac{2J}{\pi}\sum_{n,m}(-1)^{n+m}\ln[(x-2n)^2+(y-2m)^2], \quad (4.1)$$

taking $x_R=1$ as a unit length and keeping the total flux $-\int_0^x\partial_x\rho(x,y)dy=J$. Integrating $p(x)=\int_0^x\rho(x,y)dy$ and using (2.10), after numerical summation, we obtain the resulting $D(x)$ (Fig. 8), which differs significantly from the formula (1.12) for the uncut cone $D(x)=\arctan 1\simeq 0.785$ especially near the boundary $x=1$.

This calculation also probably explains why the check of the formula (1.12) by simulations of diffusion in a 3D linear cone [7] failed for $|R'|>1$. Despite the fact that the uncut cone is an exactly solvable geometry for any slope (also for 3D symmetric channels), the effect of the boundaries at the ends $x=x_{L,R}$ becomes important for steep finite cones and the real $D(x)$ differs from the formula (1.12).

Any finite channel defined on an interval $x_L<x<x_R$ can be extended by mirrors with respect to the planes placed at its ends, so we can work finally with an infinite channel of periodic boundary $A(x)=A(x+2[x_R-x_L])$ and the symmetry $A(x)=A(2x_{R,L}-x)$. Due to these symmetries, the stationary 2D (3D) density at the ends also becomes constant in $y$ and the usual BCs $\rho(x_{L,R},y)=\rho_{L,R}$ can be imposed there. If the extended periodic boundary $A(x)$ remains an analytic function, there is no problem using the mapping; at least the smooth extended boundary $[A'(x)|_{x=x_{L,R}}=0]$ allows us to use lower-order approximations like (1.12).

For nonanalytic $A(x)$, one does not expect to find any reliable universal approximate formula for $D(x)$, composed from the first few derivatives of $A(x)$. One should solve such a geometry separately, as is done, e.g., in [9,10]. The most general way is to look for the stationary density $\rho(x,\mathbf{y})$ and then, after integrating $p(x)$, to calculate $D(x)$ from the relation (2.10). In a finite channel with constant densities $\rho_{L,R}=\rho(x_{L,R},y)$ at its ends, the stationary density is equivalent to the electrostatic potential inside the channel of the perfectly dielectric walls closed by two conducting plates and charged on the potentials $\rho_L$ and $\rho_R$. One can use methods developed for solving such problems in electrostatics. Also the formulation in the complex plane does not put any restrictions on the analyticity of $A(x)$. Nonsmooth channels can be solved as well, if the corresponding $f(z)$ are found.

## V. CONCLUSION

Our analysis can be summarized as follows.

The key point is that the effective diffusion coefficient $D(x)$, as introduced in Eq. (1.6) (but unfixed) within the mesoscopic nonequilibrium thermodynamics, is a well-defined quantity in the limit of stationary diffusion (a slowly changing, but finite flux). Using the mapping procedure [4–6], we can fix $D(x)$ unambiguously in the form of an expansion in the parameter of anisotropy $\epsilon$ (the ratio of the longitudinal and the transverse diffusion coefficient) for any channel with the boundary defined by an analytic function $A(x)$. The mapping shows that then also the stationary 1D density $p(x)$ and the corresponding full-space density $\rho(x,\mathbf{y})$ are fixed up to two integration constants.

Thus, for calculating $D(x)$, we can use the stationary density $\rho(x,\mathbf{y})$, solving the Laplace equation $\Delta\rho=0$ and satisfying the Neumann BC on the walls of the channel and the Dirichlet BC at its ends. Then $D(x)$ can be expressed from the relation (2.10), after integrating $p(x)$ according to (1.3).

For an arbitrary boundary, this task is still difficult, so we proposed nonperturbative techniques for deriving approximate formulas for $D(x)$. The first one replaces the true boundary by some exactly solvable geometry in the vicinity of a chosen point $x$ and uses the corresponding $\rho(x,\mathbf{y})$ instead of the exact density. We showed that we can include $A''$ in the formula for $D(x)$ [e.g., Eq. (1.13)]. The second technique, based on variational mapping [8], optimizes the shape of surfaces of the same stationary density (isodensities) or the transformation $s=s(x,y)$ to the corresponding curvilinear coordinate system.

We tested our approximations on two exactly solvable channels and analyzed their applicability. We demonstrated that the formulas for $D(x)$ are connected with the corresponding full-space stationary density in the channel and knowing it is important for understanding reliability of the approximation.

The expansions in $\epsilon$, Eqs. (1.10) and (1.11), as well as the approximate formulas depending on the first few derivatives of $A(x)$ suppose that the function $A(x)$ is analytic. The nonanalytic points (like cusps) cause the full-space density, obtained by the backward mapping from 1D picture, to be not consistent. Similar problems can appear near the ends of finite channels if the BCs imposed at the ends are not consistent with the stationary full-space density of the corresponding infinite (uncut) channel. One should use other methods solving the Laplace equation to find $\rho(x,\mathbf{y})$ and to calculate $p(x)$ and finally $D(x)$ in such cases.

The effective diffusion coefficient $D(x)$, if defined in the limit of the stationary flow, bears information about the corresponding stationary curvilinear coordinate system in the channel. The best possible approximation of that kind, taking the exact stationary curvilinear system into account, supposes that the nonstationary density evolves only in the longitudinal curvilinear coordinate $s$. In the limit of very slow changes of the density and flux, we should get the exact results. The question of how appropriate is this description [Eq. (1.6)] for full dynamics, far from the stationary regime, is the province of future study.

## ACKNOWLEDGMENTS

Support from VEGA Grant No. 2/3107/24 and Project APVV No. 51-003505 is gratefully acknowledged.

## APPENDIX A: LINEAR CONE

We give here an example of the transformation to the curvilinear coordinate $z=z(x,y)$, calculated for the linear cone $A(x)=\gamma(x-a_0)$, which is an exactly solvable problem in the stationary diffusion. We refer here to the calculation done in the Appendix of [6].

The coefficient $D(x)=\arctan(\sqrt{\epsilon}\gamma)/\sqrt{\epsilon}\gamma$ is constant in $x$ for this geometry, so $\hat{\eta}(x,y,\partial_x)$ can be commuted in $\hat{\eta}[1/A(x)D(x)]=[1/D(x)]\hat{\eta}[1/A(x)]$. The expression $\hat{\eta}[1/A(x)]$ is known from the derivation of $D(x)$ [6]:

$$\epsilon\hat{\eta}\frac{1}{A(x)}=-\frac{1}{\gamma}\sum_{j=1}^{\infty}\left[\frac{1}{2j}\left(-\frac{\epsilon\gamma^2y^2}{A^2(x)}\right)^j-\frac{(-\epsilon\gamma^2)^j}{2j(2j+1)}\right]$$
$$=\frac{1}{\gamma}\left[1-\frac{\arctan\sqrt{\epsilon}\gamma}{\sqrt{\epsilon}\gamma}+\frac{1}{2}\ln\frac{1+\epsilon\gamma^2y^2/A^2}{1+\epsilon\gamma^2}\right]; \tag{A1}$$

hence, according to definition (2.15), $z(x,y)$ reads

$$z(x,y)=\frac{\sqrt{\epsilon}}{\arctan\sqrt{\epsilon}\gamma}\left[1-\frac{\arctan\sqrt{\epsilon}\gamma}{\sqrt{\epsilon}\gamma}+\frac{1}{2}\ln\frac{A^2+\epsilon\gamma^2y^2}{1+\epsilon\gamma^2}\right] \tag{A2}$$

plus an integration constant. We thus obtained the expected result: the curves joining the same density are ellipses (circles for $\epsilon=1$) of radius $\sqrt{(x-a_0)^2+\epsilon y^2}=r$; the stationary 2D density is then $\rho=\rho_L-(\sqrt{\epsilon}J/\arctan\sqrt{\epsilon}\gamma)\ln r$. If (A2) is expanded in $\epsilon$ and $y^2$, we get the coefficients (2.17).

## APPENDIX B: COMPLEX PLANE METHOD

The stationary density satisfies the Laplace (mass conservation) equation $\Delta\rho(x,y)=0$, so for solving it, we can apply methods used in electrostatics. In this appendix, we formulate this problem in the complex plane, which enables us to complete the calculation of $D(x)$ for 2D channels in a very concise way.

Let us consider an analytic function $f(z)$ of the complex variable $z$:

$$Jf(z)=Jf(x+iy)=\varphi(x,y)+i\rho(x,y). \tag{B1}$$

The Cauchy-Riemann conditions

$$\partial_x\varphi(x,y)=\partial_y\rho(x,y),\quad \partial_y\varphi(x,y)=-\partial_x\rho(x,y) \tag{B2}$$

tell us that both $\varphi(x,y)$ and $\rho(x,y)$ satisfy the Laplace equation and also that the curves $\varphi=\varphi(x,y)$ and $\rho=\rho(x,y)$ with constant $\varphi$ and $\rho$ are orthogonal; $\nabla\varphi(x,y)\cdot\nabla\rho(x,y)=0$. So, if we choose $\rho(x,y)$ to satisfy the Neumann BC on the boundaries $y=0$ and $A(x)$, $\varphi(x,y)$ has to be constant along them. We can now identify $\rho(x,y)$ as the 2D stationary density and $\varphi=\varphi(x,y)$ corresponds to the transverse curvilinear coordinate, orthogonal to $\rho$, as mentioned in Sec. II.

The value of $\varphi(x,0)$ can be set to zero; then, $\varphi(x,A(x))$ is fixed by the definition of the total flux $J$:

$$\begin{aligned} J &= -\int_0^{A(x)} \partial_x \rho(x,y)dy \\ &= -\frac{J}{2i}\int_0^{A(x)} [\partial_x f(x+iy) - \partial_x f(x-iy)]dy \\ &= \frac{J}{2}\int_0^{A(x)} [\partial_y f(x+iy) + \partial_y f(x-iy)]dy = \varphi(x,A(x)), \end{aligned} \tag{B3}$$

so the function $f(z)$, corresponding to the stationary density inside a channel bounded by $y=A(x)$ and the $x$ axis, has to satisfy the equations

$$\mathrm{Re}f(x) = 0 \quad \text{and} \quad \mathrm{Re}f[x+iA(x)] = 1. \tag{B4}$$

Knowing the solution $f(z)$, its primitive function $g(z) = \int f(z)dz$ enters the formula for 1D density $p(x)$:

$$\begin{aligned} p(x) &= \int_0^{A(x)} \rho(x,y)dy = J\int_0^{A(x)} \mathrm{Im}[g'(x+iy)]dy \\ &= J\int_0^{A(x)} \mathrm{Im}\left[\frac{1}{i}\partial_y g(x+iy)\right]dy \\ &= -J\mathrm{Re}[g(x+iA(x)) - g(x)], \end{aligned} \tag{B5}$$

so the definition (2.10) finally results in

$$\frac{1}{D(x)} = A(x)\frac{d}{dx}\left(\frac{1}{A(x)}\mathrm{Re}[g(x+iA(x)) - g(x)]\right). \tag{B6}$$

We can easily test both the LA and CA. Taking Eq. (3.2) for the density in the linear cone $A(x)=\gamma(x-a_0)$ and rewriting it in terms of $z=x+iy$ and $\bar{z}=x-iy$,

$$\begin{aligned} \rho(x,y) &= \rho_L - \frac{J}{2\arctan\gamma}\ln[(x-a_0)^2+y^2] \\ &= \rho_L - \frac{J}{2\arctan\gamma}\ln(z-a_0)(\bar{z}-a_0), \end{aligned} \tag{B7}$$

we obtain

$$f(z) = f(x+iy) = \frac{-i}{\arctan\gamma}\ln\frac{x+iy-a_0}{r_0}, \tag{B8}$$

whose imaginary part reproduces (B7) ($\rho_L$ is replaced by the length scale $r_0$) and the real part gives $\varphi$,

$$\varphi(x,y) = \frac{J}{\arctan\gamma}\arctan\frac{y}{x-a_0}, \tag{B9}$$

which is proportional to the angle in the cone. Calculating the function $g(z)$,

$$g(z) = \frac{-i}{\arctan\gamma}\left[(z-a_0)\ln\left(\frac{z-a_0}{r_0}\right) - z\right], \tag{B10}$$

and substituting it into Eq. (B6), one arrives at the LA (1.12).

The circular approximation is based on the model of a couple of source and sink at points $(\mp w,0)$, which is equivalent to a couple of opposite charges in electrostatics, placed at $(\mp w,0)$ and interacting by the 2D logarithmic Coulomb potential. So $\rho(x,y)$ (equivalent to the potential from both charges) is

$$\begin{aligned} \rho(x,y) &= -\frac{J}{2\arctan\gamma}\ln\frac{(w+x)^2+y^2}{(w-x)^2+y^2} \\ &= -\frac{J}{2\arctan\gamma}\ln\frac{(w+z)(w+\bar{z})}{(w-z)(w-\bar{z})}, \end{aligned} \tag{B11}$$

if rewritten in the complex variables $z,\bar{z}=x\pm iy$. Then we have the corresponding function $f(z)$ in the form

$$f(z) = \frac{-i}{\arctan\gamma}\ln\frac{w+z}{w-z}. \tag{B12}$$

The circular isodensities, given by the equation

$$(x+w/s)^2 + y^2 = (1/s^2-1)w^2 \tag{B13}$$

coming from (B11), define a longitudinal curvilinear variable $s=\tanh[(\arctan\gamma)\rho/J]$, which is orthogonal to

$$\varphi = J\,\mathrm{Re}[f(z)] = \frac{J}{\arctan\gamma}\arctan\frac{2wy}{w^2-x^2-y^2}. \tag{B14}$$

From (B14), the lines of constant $\varphi$ are also circles,

$$x^2 + (y+w\sigma)^2 = (1+\sigma^2)w^2, \tag{B15}$$

now centered on the $y$ axis; $\sigma=\tan[(\arctan\gamma)\varphi/J]$. By setting $\gamma$, we choose a circle (B15) of $\sigma=\gamma$, for which the condition $\varphi=J$, Eq. (B4), is satisfied, and thus it can serve as a boundary of our channel.

The coordinate system can be shifted by any $x_0$ in the $x$ direction, so we can work with the function

$$f(z) = \frac{-i}{\arctan\gamma}\ln\frac{w-x_0+z}{w+x_0-z} \tag{B16}$$

of three parameters $w$, $\gamma$ (related to $y_0$ and $R_0$), and $x_0$, allowing us to fit $A$, $A'$, and $A''$ of the true boundary at a chosen $x=\bar{x}$. If integrated in $z$, we get

$$g(z) = \frac{-i}{\arctan\gamma}\left[(z-x_0)\ln\left(\frac{w-x_0+z}{w+x_0-z}\right) + \ln[w^2-(z-x_0)^2]\right], \tag{B17}$$

and after substituting into (B6), we restore the CA formula (3.11) before replacing $x_0$, $y_0$, and $R_0$ by $A$ and its derivatives.

In general, the crucial problem is to solve Eqs. (B4) to find $f(z)$ for an arbitrary $A(x)$. Our method inverts this task; for a chosen ansatz for $f(z)$, becoming imaginary at the real axis, we look for the line $y=A(x)$, where $\mathrm{Re}f(z)=1$. If we find such an ansatz, depending on a set of parameters $\{a_0,a_1,\ldots,a_n\}$, which enables us to express analytically the relations between $a_j$ and the corresponding $A(x)$ and its first $n$ derivatives at a point $x=\bar{x}$, then $D(x)$, depending on the $a_j$ as calculated from Eq. (B6), can be rewritten using the derivatives of $A(x)$, yielding the formula for a higher-order approximation.

The function (B16) can be taken as an example of such an ansatz with the parameters $x_0$, $w$, and $\gamma$, yielding the CA. Another interesting ansatz is

$$f(z) = \frac{-i}{\arctan \gamma} \ln\left(\frac{z+\sqrt{z^2+a^2}}{a}\right), \tag{B18}$$

fixing the hyperbolic boundary

$$A(x) = \gamma\sqrt{x^2 + a^2/(1+\gamma^2)} \tag{B19}$$

from the condition $\mathrm{Re}[f(z)]=1$; $\gamma$ characterizes the opening of the cone and $a$ is the transverse length unit. The corresponding isodensities are ellipses

$$x^2/\sinh^2 s + y^2/\cosh^2 s = a^2 \tag{B20}$$

for any $\gamma$; $s$ denotes a longitudinal curvilinear coordinate, related to the stationary density $\rho$. We gain $g(z)$ by integrating (B18), and after substituting into (B6), we obtain

$$\frac{1}{D(x)} = 1 + \frac{\gamma^2 x^2}{A^2(x)}\left(\frac{\gamma}{\arctan \gamma} - 1\right), \tag{B21}$$

which is used in Sec. III for testing the other approximations.

Also, here, we can shift the coordinate system by $x_0$ in the $x$ direction and earn the third parameter for fitting the general boundary. Taking Eq. (B19) with $x$ replaced by $x-x_0$ and its first two derivatives, we get equations for $a$, $\gamma$, and $x_0$, allowing us to express them using $A$, $A'$, and $A''$ of the true boundary at $x=\bar{x}$:

$$\gamma^2 = A'^2 + AA'', \quad \bar{x} - x_0 = \frac{AA'}{A'^2 + AA''},$$

$$a^2 = \frac{A^3 A''(1 + A'^2 + AA'')}{(A'^2 + AA'')^2}. \tag{B22}$$

Substituting for these parameters into (B21) with $x$ shifted by $x_0$, we derive the approximating formula

$$\frac{1}{D(x)} = 1 + \frac{A'^2}{A'^2 + AA''}\left(\frac{\sqrt{A'^2 + AA''}}{\arctan \sqrt{A'^2 + AA''}} - 1\right), \tag{B23}$$

which also involves $A''$. If $A$ and its derivatives are rescaled by $\sqrt{\epsilon}$, we can expand it in $\epsilon$:

$$D(x) = 1 - \frac{\epsilon}{3}A'^2 + \frac{\epsilon^2}{45}A'^2(9A'^2 + AA'') - \frac{\epsilon^3}{945}A'^2 \times (135A'^4 + 144AA'^2A'' + 44A^2A''^2) + \cdots. \tag{B24}$$

In contrast to the CA, this expansion does not recover the terms proportional to $A''$ in the exact expansion (1.10).

Finally, we examine the polynomial ansatz

$$f(z) = -i\sum_{j=0}^{n} a_j z^j, \tag{B25}$$

enabling us to introduce more than three parameters $a_j$. In its simplest form $n=2$, the equation $\mathrm{Re}[f(z)]=a_1 y + 2a_2 xy = 1$ defines the hyperbolic boundary

$$y = A(x) = 1/(a_1 + 2a_2 x); \tag{B26}$$

the density $\rho(x,y)=\mathrm{Im}[f(z)]=-[a_0+a_1x+a_2(x^2-y^2)]$ forms hyperbolic isodensities

$$(x + a_1/2a_2)^2 - y^2 = (a_1/2a_2)^2 - (\rho + a_0)/a_2 \tag{B27}$$

in the channel. The function $g(z)$,

$$g(z) = \int f(z)dz = -i\sum_{j=0}^{n} \frac{1}{j+1} a_j z^{j+1}, \tag{B28}$$

gives $\mathrm{Re}[g(x+iy)]=(a_0+a_1x+a_2x^2)y-a_2y^3/3$ in this case, so after substituting into (B6), we get

$$\frac{1}{D(x)} = 1 + \frac{4a_2^2}{3(a_1 + 2a_2x)^4} = 1 + \frac{1}{3}A'^2(x); \tag{B29}$$

$a_1$ and $a_2$ were expressed using $A(x)$, Eq. (B26), and its derivative; i.e., the real boundary is replaced by the hyperbola (B26) at a chosen $x$. There are only two effective parameters here, so we can include only $A'$ (and $A$) into $D(x)$. Including higher derivatives in $D(x)$ requires taking larger $n$. For $n=3$, solution of the equation

$$\mathrm{Re}[f(x)] = (a_1 + 2a_2x + 3a_3x^2)y - a_3y^3 = 1 \tag{B30}$$

defines the boundary $y=A(x)$ of a complicated form, but we do not need to know it explicitly. The real part of $g(x+iA(x))$, Eq. (B28), for $n=3$, substituted into (B6), gives

$$\frac{1}{D(x)} = A(x)\left(u(x) - \frac{1}{3}u'(x)A(x)A'(x) - a_3A^2(x)\right), \tag{B31}$$

where $u(x)=a_1+2a_2x+3a_3x^2$. Now, we express the functions $u(x)$, $u'(x)$, and $a_3=u''(x)/6$ using $A$, $A'$, and $A''$ directly from (B30); solving $u(x)A(x)-a_3A^3(x)=1$ and its two derivatives yields

$$u = \frac{3(2 - AA'')}{2A(3 - A'^2 - AA'')}, \quad u' = \frac{3A'(A'^2 - 1)}{A^2(3 - A'^2 - AA'')},$$

$$a_3 = \frac{2A'^2 - AA''}{2A^3(3 - A'^2 - AA'')}. \tag{B32}$$

Substituting it into (B31), we get

$$D(x) = \frac{3 - A(x)A''(x) - A'^2(x)}{3 - A(x)A''(x) - A'^4(x)}. \tag{B33}$$

The same treatment can be used also for higher $n$. Fixing $a_j$ to fit the boundary at a point $x$ requires us to solve the system of equations (B4) for Eq. (B25), and its first $n-1$ derivatives, which are linear in $a_j$ and so solvable for any $n$. Taking $n=4$ gives the formula (3.17).

For testing our approximations, we use the exactly solvable geometry defined by the function

$$f(z) = -\frac{i}{g}\sinh z. \tag{B34}$$

The condition (B4) yields the corresponding boundary

$$y = A(x) = \arcsin\left(\frac{g}{\cosh x}\right); \tag{B35}$$

$0 < g \leqslant 1$. From the function $g(z) = -(i/g)\cosh z$, using the formula (B6), we derive the exact $D(x)$, Eq. (3.21).

## APPENDIX C: VARIATIONAL MAPPING

In calculation of $D(x)$, the variational method helps to optimize an ansatz for the curvilinear coordinate $s = s(x,y)$, defining the (stationary) isodensities in a channel. For an exactly solvable geometry, there is no problem to take directly $s = z$, Eq. (2.15), which is known explicitly, but in general, we know the coefficients (2.17) of its expansion (2.16) in $\epsilon$ only up to a finite order. So we try to construct a variable $s$ independently of this expansion, supposing that $s = s(z)$ and thus also the 2D stationary density $\rho(x,y) = \rho(s)$. Then the BCs (2.1) have to be satisfied

$$\rho'(s)\partial_y s(x,y) = 0\big|_{y=0},$$

$$\rho'(s)\partial_y s(x,y) = \epsilon\rho'(s)A'(x)\partial_x s(x,y)\big|_{y=A(x)} \tag{C1}$$

[$\rho'(s)$ becomes irrelevant here], and the stationary mass conservation $[\partial_x^2 + (1/\epsilon)\partial_y^2]\rho(s(x,y)) = 0$ becomes

$$\rho''(s)\left((\partial_x s)^2 + \frac{1}{\epsilon}(\partial_y s)^2\right) + \rho'(s)\left(\partial_x^2 + \frac{1}{\epsilon}\partial_y^2\right)s = 0. \tag{C2}$$

Here, $\rho'(s)$ will be expressed as the stationary solution of Eq. (3.24), using $\kappa(s)$. It depends on $x(s,y)$, Eq. (3.25), inverse to $s(x,y)$, and so the condition (C2) fixing $s(x,y)$ becomes closed, too. We demonstrate this construction in the following calculations. For comparison with the perturbation expansion, we keep the parameter of anisotropy $\epsilon$ unequal to 1.

### 1. Circular isodensities

We begin with an ansatz $s = s(x,y)$, describing isodensities as circles, which are consistent with the LA and CA. Let us define the variable $s$ as the $x$ coordinate of the intersection of the corresponding isodensity with the boundary; $s = s(x = s, y = A(s))$. To keep the BC (2.1) at $y = 0$, the circles have to be centered on the $x$ axis. Then the relation $s = s(x,y)$, expressed implicitly as

$$[x - a_0(s)]^2 + \epsilon y^2 = [s - a_0(s)]^2 + \epsilon A^2(s), \tag{C3}$$

complies with all these requirements. The only parameter $a_0(s)$ is fixed to fit the BC. Completing the derivatives of (C3) and substituting for $\partial_x s$, $\partial_y s$ in (C1), we obtain

$$a_0(s) = s - A(s)/A'(s); \tag{C4}$$

a similar relation to (3.1) for the linear cone, but now the position of the center $a_0(s)$ changes along the channel, to set the correct BC for any circle $s = s(x,y)$.

Our next step is to calculate the stationary 2D density $\rho(x,y) = \rho(s)$ from Eq. (3.24). In the stationary state $\partial_t \rho = 0$, the coefficient $\alpha(s)$ becomes irrelevant and $\rho(s)$ can be immediately integrated:

$$\rho(s) = \rho_L - J\int \frac{ds}{\kappa(s)}; \tag{C5}$$

$\rho_L$ and $J$ stand for the integration constants. [Equation (3.24) represents the mass conservation law for the 1D density $\bar{\rho}(s)$ in the curvilinear system, calculated at a given $s$: $\bar{\rho}(s,t) = \int_0^{A(s)} dy(\partial_s x)\rho(s(x,y),t) = \alpha(s)\rho(s)$. So $-\kappa(s)\rho'(s) = J$ has to be the total flux, which is the same, whether integrated over the cross section either at constant $s$ or at constant $x$.]

The coefficient $\kappa(s)$, Eq. (3.25), requires us to express the inverse relation $x = x(s,y)$, which can be easily done for our definition of $s$:

$$x = s + \frac{1}{A'(s)}\{\sqrt{A^2(s) + \epsilon A'^2(s)[A^2(s) - y^2]} - A(s)\}; \tag{C6}$$

the integration in (3.25) can be also carried out explicitly, with the upper limit $A(x_s) = A(s)$. Then

$$\kappa(s) = \frac{A(s)[1 + \epsilon A'^2(s)]\arctan\sqrt{\epsilon}\gamma(s)}{[1 + \epsilon A'^2(s) + \epsilon A(s)A''(s)]\sqrt{\epsilon}\gamma(s)}, \tag{C7}$$

where

$$\sqrt{\epsilon}\gamma(s) = \frac{\sqrt{(1 + \epsilon A'^2)^3 - (1 + \epsilon A'^2 + \epsilon AA'')^2}}{1 + \epsilon A'^2 + \epsilon AA''}. \tag{C8}$$

The integration of the inverted $\kappa(s)$ in (C5) cannot be completed analytically for a general $A(s)$, so we have to make another approximation. One possibility is to approximate the boundary in the vicinity of some $x$ by a function that makes $\arctan\sqrt{\epsilon}\gamma(s)$ in (C7) constant. This requirement is satisfied by the ellipses

$$\epsilon[A(s) - y_0]^2 + (s - x_0)^2 = R_0^2, \tag{C9}$$

solving the differential equation $\gamma(s) = \gamma = \text{const}$; $x_0$, $y_0$, and $R_0$ are constant, connected with two integration constants and $\gamma$. Differentiating (C9) twice, we get

$$A'(s) = \frac{-(s - x_0)}{\epsilon(A(s) - y_0)}, \quad A''(s) = \frac{-R_0^2}{\epsilon^2(A(s) - y_0)^3}, \tag{C10}$$

which fixes $\gamma$ after substituting into (C8):

$$\gamma = \sqrt{R_0^2 - \epsilon y_0^2}/(-\epsilon y_0). \tag{C11}$$

Now, $\kappa(s)$ has the simplified form

$$\kappa(s) = \frac{\sqrt{\epsilon}A(s)|A(s) - y_0|}{\sqrt{R_0^2 - \epsilon y_0^2}}\arctan\sqrt{\epsilon}\gamma, \tag{C12}$$

and if $A(s)$ is expressed from (C9), the integration in (C5) can be carried out explicitly:

$$\rho(s) = \rho_L - \frac{\sqrt{\epsilon}J}{2\arctan\sqrt{\epsilon}\gamma} \times \ln\frac{R_0^2 - \sigma\sqrt{\epsilon}y_0\sqrt{R_0^2-(s-x_0)^2} + w(s-x_0)}{R_0^2 - \sigma\sqrt{\epsilon}y_0\sqrt{R_0^2-(s-x_0)^2} - w(s-x_0)}; \tag{C13}$$

$\sigma=\mathrm{sgn}[A''(s)]$ and $w$ abbreviates $\sqrt{R_0^2-\epsilon y_0^2}$.

For $A(s)$ approximated by the ellipse (C9), we can express $s$ from (C3) explicitly and rewrite the stationary $\rho(s)$ in the Cartesian coordinates; putting $\epsilon=1$, we arrive at the relation (3.9). Then the calculation of $D(x)$ continues in the same way as in Sec. III. The ellipses (C9) are equivalent to the approximating circular boundary (3.5) for $\epsilon=1$ and $s=x$; hence, we get the same relations between the constants $x_0$, $y_0$, $R_0$ and $A$, $A'$, $A''$ at $x=\bar{x}$, and finally the formula (3.11) for $D(x)$.

Supposing circular isodensities (C3) and the simplifying condition $\gamma(s)=\gamma=$const, Eq. (C8), we recover the CA; a simpler condition neglecting $A''$ in (C8) gives $\gamma(s)=|A'(s)|$ and leads to the LA.

### 2. Generalization of the method

Achieving better approximations for $D(x)$ requires finding a more sophisticated ansatz for system of isodensities than the circles. We formulate here some rules helping us to choose such an ansatz and to estimate the precision which can be reached with it.

In general, the inverse transformation $x=x(s,y)$ can be written in the form

$$x(s,y) = \sum_{j=0}^{\infty}\epsilon^j\sum_{k=0}^{j} x_{j,k}(s)y^{2k}, \tag{C14}$$

which is inverse to the expansion (2.16) and so it is able to fit both the BC (C1) and the stationary mass conservation (C2). To express $\kappa(s)$, Eq. (3.25), in a usable form, we retain the definition of $s$ as the $x$ coordinate of intersection of the corresponding isodensity with the boundary $y=A(x)$. Then the form of $x(s,y)$, Eq. (C14), reduces to

$$x(s,y) = s + (A^2(s)-y^2)\sum_{j=1}^{\infty}\epsilon^j\sum_{k=1}^{j}\bar{x}_{j,k}(s)y^{2k-2},$$

satisfying the condition $x(s,y=A(s))=s$; the upper limit $A(x_s)$ of the integrals in (3.25) becomes $A(s)$.

The next restriction is given by the BC (C1). If it is rewritten using the inverse relation, $\partial_x s(x,y)=1/\partial_s x(s,y)$ and $\partial_y s(x,y)=-\partial_y x(s,y)/\partial_s x(s,y)$, we get

$$\partial_y x(s,y)|_{y=A(s)} = -2A(s)\sum_{j=1}^{\infty}\epsilon^j\sum_{k=1}^{j}\bar{x}_{j,k}(s)A^{2k-2}(s) = -\epsilon A'(s), \tag{C15}$$

so finally the ansatz for $x(s,y)$ of the form

$$x = s + \epsilon\xi_{1,1}(s)[A^2(s)-y^2] + \sum_{j=2}^{\infty}\epsilon^j\sum_{k=2}^{j}\xi_{j,k}(s)[A^2(s)-y^2]^k, \tag{C16}$$

with

$$\xi_{1,1}(s) = A'(s)/2A(s) \tag{C17}$$

also fits the boundary condition. The remaining coefficients $\xi_{j,k}$ are to be fixed by the mass conservation law. The operator $\Delta_\epsilon=\partial_x^2+(1/\epsilon)\partial_y^2$ is expressed in the coordinates $s$ and $y$,

$$\Delta_\epsilon = \left[\left(\frac{\partial x}{\partial s}\right)^{-1}\partial_s\right]^2 + \frac{1}{\epsilon}\left[\partial_y - \frac{\partial x}{\partial y}\left(\frac{\partial x}{\partial s}\right)^{-1}\partial_s\right]^2, \tag{C18}$$

and applied on $\rho(s)$. Taking into account that $\rho'(s)=-J/\kappa(s)$, we have the condition

$$\left\{\frac{1}{\epsilon}\left[\frac{\partial x}{\partial y}\left(\frac{\partial x}{\partial s}\right)^{-1}\partial_s - \partial_y\right]\frac{\partial x}{\partial y} + \left(\frac{\partial x}{\partial s}\right)^{-1}\partial_s\right\}\left(\frac{\partial x}{\partial s}\kappa(s)\right)^{-1} = 0. \tag{C19}$$

Now, $\kappa(s)$ is calculated according to (3.25) using $x(s,y)$ in the form (C16). Finally, the expansion of the left-hand side of (C19) in $\epsilon$ and $y^2$ gives the conditions fixing unambiguously $\xi_{j,k}$; e.g., in $\epsilon^1$, we get

$$\xi_{2,2}(s) = \frac{A^{(3)}(s)}{24A(s)} - \left(\frac{A'(s)}{2A(s)}\right)^3. \tag{C20}$$

The circular isodensities used in the LA and CA have the form (C16). If the relation (C6) is expanded in $\epsilon$,

$$x = s + \epsilon\frac{A'(s)}{2A(s)}[A^2(s)-y^2] - \epsilon^2\frac{A'^3(s)}{8A^3(s)}[A^2(s)-y^2]^2 + \cdots, \tag{C21}$$

the coefficients of $\epsilon^1$ and $\epsilon^2$ recover $\xi_{1,1}$ and $\xi_{2,2}$ up to $A''$, which is the precision achieved by setting the only parameter $a_0(s)$ in (C3), to satisfy the BC. The next improvements need to choose a curve with more parameters than a circle, to fit independently more $\xi_{j,k}$. The analysis presented restricts the choice of ansatz, fixes its free parameters, and shows the precision that can be reached.

Having an ansatz $x=x(s,y)$, we need to integrate $\kappa(s)$ according to (3.25), the density $\rho(s)$, Eq. (C5), to switch to Cartesian coordinates and to find $p(x)$. The results of these three integrations should be expressed analytically in order to get the final formula for $D(x)$ from (2.10) in a compact form. This procedure presumably cannot be completed for general $A(x)$; one has to make another approximation(s) during this calculation. One way is to approximate $A(x)$ by a function for which $1/\kappa(s)$ becomes integrable, as is demonstrated for the CA. Then this analysis becomes complementary to the method replacing the true boundary by an exactly solvable geometry, as described in Sec. III.

[1] M. H. Jacobs, *Diffusion Processess* (Springer, New York, 1967).
[2] R. Zwanzig, J. Phys. Chem. **96**, 3926 (1992).
[3] D. Reguera and J. M. Rubí, Phys. Rev. E **64**, 061106 (2001).
[4] P. Kalinay and J. K. Percus, J. Chem. Phys. **122**, 204701 (2005).
[5] P. Kalinay and J. K. Percus, J. Stat. Phys. **123**, 1059 (2006).
[6] P. Kalinay and J. K. Percus, Phys. Rev. E **74**, 041203 (2006).
[7] A. M. Berezhkovskii, M. A. Pustovoit, and S. M. Bezrukov, J. Chem. Phys. **126**, 134706 (2007).
[8] P. Kalinay and J. K. Percus, Phys. Rev. E **72**, 061203 (2005).
[9] A. M. Berezhkovskii, V. Yu. Zitserman, and S. Y. Shvartsman, J. Chem. Phys. **118**, 7146 (2003).
[10] A. M. Berezhkovskii, V. Yu. Zitserman, and S. Y. Shvartsman, J. Chem. Phys. **119**, 6991 (2003).